

Advanced MRI

CHAPTER 10

MRI and PLANTS

H. Van As

Introduction

One of the least well understood aspects of plant physiology is the integration and co-ordination of processes at the organ and whole plant level. This deficiency is scarcely surprising; technological developments that would make it possible to routinely and accurately measure performance of the whole plant have received little attention. Mechanism and control of water and solute fluxes in the xylem and the phloem are examples of such processes, essential for understanding important mechanisms such as elongation growth, fruit development and growth inhibition by e.g. drought stress and fungal infection. By being able to measure these fluxes in relation to the plant (cell) water balance and the cell-to-cell transport it will be possible to explicitly or implicitly examine many aspects of plant function.

NMR is increasingly applied to the study of plant cells, plant organs and living plants. When applying NMR to plants one has to deal with structural and physiological features that are different from those in animals at all levels of biological complexity, from the macromolecule to the organs. Additional compartments such as the chloroplast, the vacuole or the periplasm and unique physiological features, such as photosynthesis or assimilation of various inorganic ions, impose specific constraints on the measurements and require careful physiological control.

Susceptibility

Plant tissue includes intercellular air spaces in the order of 10 to 100 μm , resulting in local magnetic field gradients, $\langle g_z^2 \rangle$, or susceptibility artefacts. These artefacts strongly depend on the magnetic field strength and increase with increasing field strength: $\langle g_z^2 \rangle (\text{:}) B_0^2$. These susceptibility artefacts limit the resolution in MRI and NMR spectroscopy. This is the reason for the use of as short as possible echo times in high field microscopic ^1H imaging of plant material (see below). Alternatively, air spaces can be removed by vacuum infiltration of the plant tissue with a liquid medium. Susceptibility artefacts may also play a dominant role in imaging roots in soil. This problem cannot be solved by vacuum infiltration. Therefore, artificial root media have been suggested for the improvement of root imaging.

Effect of diffusion on T_2

Multi-echo imaging (see Figure 1) results in quantitative T_2 and spin density images (see Chapter 9). However, the actually observed T_2 value depends on a number of contributions:

$$1/T_{2,\text{obs}} = 1/T_2 + 1/T_2' + 1/T_2'' \quad [1]$$

Here T_2 represents the original T_2 of the liquid in the tissue, T_2' and T_2'' originates from diffusion effects.

Diffusion through local field gradients originating from susceptibility effects leads to a rapid signal dephasing and apparently short T_2 value:

$$1/T_2' (\cdot) \gamma^2 \langle g_z^2 \rangle TE^2 D \quad [2]$$

where D is the diffusion constant. Minimizing this effect can be achieved by imaging at low magnetic field strength and at short TE values.

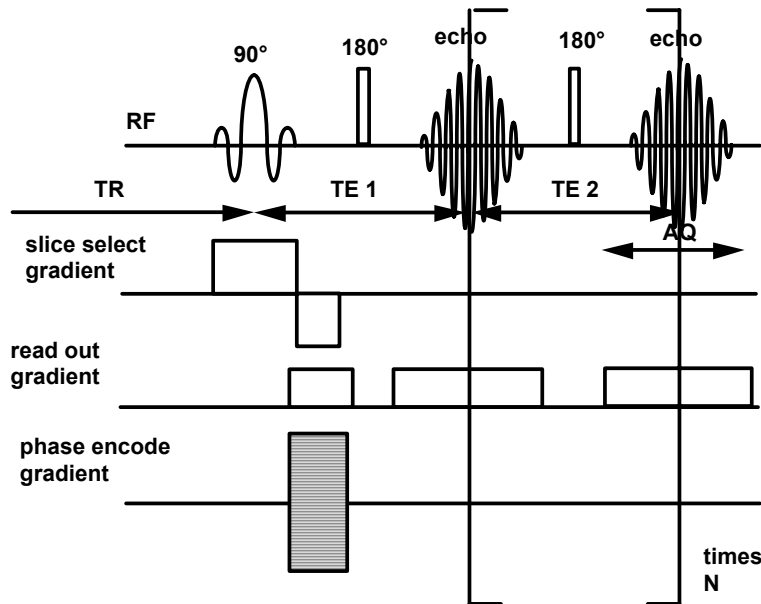


Figure 1. Schematical pulse sequence for multi-echo imaging. TE 1 and TE 2 may be different in size. The echoes can be acquired separately to obtain images with different T₂ weighting and can be used to calculate local T₂s or the echoes can be added to obtain a higher signal to noise for the images.

In addition, diffusion through the repeatedly applied read out gradients in a multi-echo experiment contribute to the observed relaxation time:

$$1/T_2'' = \gamma^2 G^2 \delta^2 (1 - 4\delta/3TE) D \quad [3]$$

where 2δ is the duration of the applied read gradient. In practice, G and δ are dictated by the choice of pixel resolution, image size and TE. It follows that to image relaxation times in the order of 1 s a lower limit of 100 μ m for the pixel size can be used. At smaller pixel sizes the diffusive attenuation in the read gradients becomes the leading contribution to the observed transverse relaxation times and the information available from the actual T₂ is lost.

The effect of susceptibility is (extremely?) manifest in mushrooms. Inside the mushroom air spaces are abundant and large susceptibility effects are expected. At a magnetic field strength of 0.47 T the transverse relaxation could be characterised from a large number of echoes and the correct water distribution was obtained by extrapolation of the decay curve to zero time. A slight decrease of T₂ values was observed with longer echo times TE. However, at high fields (4.7 and 9.4 T) T₂ values were very short and decrease with increasing TE values. The actual water distribution could not be reproduced at all. Susceptibility effects could be removed by vacuum infiltration with a Gd-DTPA solution. At high concentration the T₂ of this solution is too short to be observed in the images and images of the mushroom itself was observed, with identical water distribution and longer T₂ values as observed before vacuum infiltration.

Information available

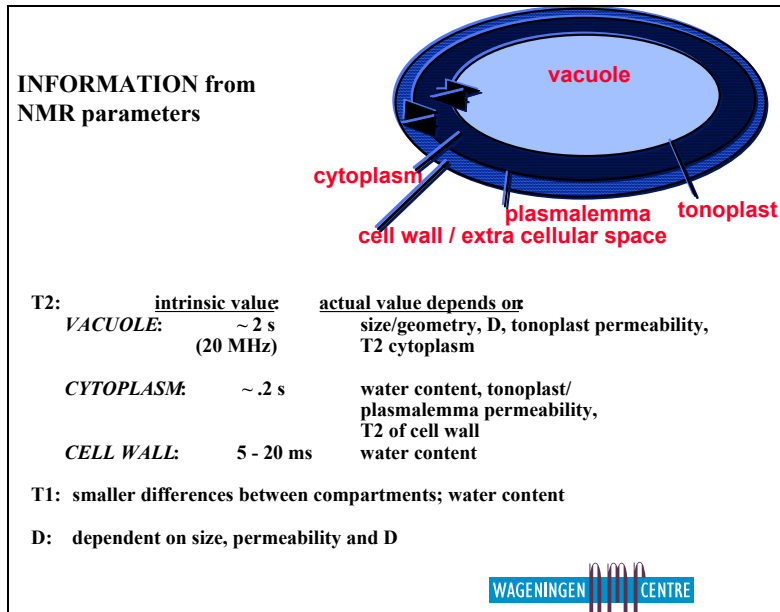
The information content and contrast of the MR images can be manipulated to represent parameters of physical or metabolic processes. In this way a combination of anatomical and physiological (functional) information is obtained, referred to as functional imaging. An example of this functional information is the molecular displacement of water molecules. This type of imaging we refer to as dynamic imaging. Other examples are the signal amplitude – representing the amount of protons: proton density per volume = proton density times water content – the relaxation times T_1 and T_2 , the diffusion constant, D , which can also be determined as a diffusion tensor, and magnetisation transfer effects.

Quantitative images can be made representing each of these parameters. This information is used for functional imaging. As a result of the relatively low spatial resolution, most pixels will contain information that originates from different sub-cellular compartments (or even cells). This is called the partial volume problem. Therefore the information presented mostly is called “apparent”: e.g. apparent T_2 or apparent D .

Information available from relaxation times

Some general observations of water relaxation in (vacuolated) plant material are that the observed T_2 is much shorter than T_1 , that T_2 in plants is shorter or even much shorter than in pure water, and that in general multi-exponential decay curves are observed. In biological systems multi-exponential relaxation has been used to obtain information on the relative proportions of water in different environments or in different physical states, e.g. "bound" and "free". In the same way, water and oil fractions have been discriminated in e.g. oil containing seeds. In addition, the solid protons of the biomass have very short T_2 values (10 - 20 μ s) and can be discriminated from the water protons. This allows the measurement of the total absolute water and oil content.

There exists a good, though not always quantitative, correlation between the NMR data and the classical measurements of water content, relative water content, tissue hydration and water potential. For the T_1 data the correlation with water content and water potential has been suggested to be high, whereas for T_2 data this correlation is more complex. Depending on experimental parameters (magnetic field strength, echo time (2τ or TE), number of data points, signal to noise ratio (S/N)) two or three exponentials are observed, which can be assigned more or less uniquely to either water in the vacuole (longest T_1 and T_2), cytoplasm ($T_1 > T_2$), and cell wall/extra cellular space (T_2 depends strongly on the water content in this compartment, and ranges from about 5 ms and higher). Within these compartments diffusive exchange results in single exponential behaviour. Due to exchange of water protons with protons of the biomass (having a small chemical shift difference with respect to water), the intrinsic T_2 values in the compartments depend on the magnetic field strength. This is manifest especially for the vacuolar water.



Proton exchange over the plasmalemma and the tonoplast membrane affects the observed relaxation times (see Fig. 2). Due to the effect of the exchange, which depends on the difference in the relaxation times in the exchanging compartments, T_1 and T_2 results are in general different, even for the number of observed exponentials. For T_1 , exchange between the compartments results in averaging, and therefore T_1 values relate with water content more uniquely. The observed T_2 of the vacuolar water depends on the vacuole size/geometry, the diffusion coefficient of the vacuole, the proton tonoplast permeability and the difference in relaxation times in the vacuole and the cytoplasm.

Restricted diffusion and diffusion tensor

The diffusion coefficient in the different cell compartments can be measured by NMR (self)diffusion measurements using Pulsed Field Gradient (PFG) NMR techniques (see Chapter 9). The diffusion measurements can be done by varying the observation time, resulting in the distance over which the spins can diffuse freely and in the permeability of the surrounding wall (membranes). In this way the size of e.g. the vacuoles in vacuolated plant tissue has been measured.

More recently, diffusion-weighted MRI has been used to study the structural characteristics of tissue. Tissues and organs that have an ordered structure, e.g. skeletal and cardiac muscle or fibers and transport vessels in plants, exhibit a dependence of the diffusivity on the direction in which the diffusion gradient(s) are applied. The spatial dependence of this diffusion anisotropy can be quantitatively studied with PFG MRI sequences, thereby providing important information about the architecture of normal and pathological tissue. To obtain a quantitative diffusion tensor image, at least six D maps must be generated, for instance for the relative gradient directions of $(G_x, G_y, G_z) = (0,0,1)$, $(0,1,0)$, $(1,0,0)$, $(0,1/\sqrt{2}, 1/\sqrt{2})$, $(1/2\sqrt{2}, 0, 1/2\sqrt{2})$, and $(1/2\sqrt{2}, 1/2\sqrt{2}, 0)$. For each D image it is advised that at least four diffusion-weighted images are acquired, such that a minimum of twenty four diffusion-weighted images needs to be generated.

Functional plant imaging

All above-mentioned information can be measured spatially resolved in any selected part of the material under observation by NMR imaging. In this way anatomical and functional information, and even functional anatomical information, is obtained. Its value for

internal quality assessment of fruits and vegetables has been investigated, turning out that voids, pits, bruises, worm, dry regions can well be observed. In addition studies on the evaluation of maturation and stage of ripeness, as well as senescence and fungal infection have been performed.

Functional imaging of intact plants has been demonstrated by combined PFG-Multi Spin Echo (PFG-MSE), PFG-TSE and Inversion Recovery-MSE imaging. Single parameter images were obtained from the MSE-experiments by assuming mono-exponential relaxation decay in each pixel. The resulting images were: signal amplitude or spin density, T_2 , and T_1 (the latter in the case of IR-MSE) and D_{app} . The propagators of each pixel obtained by fast dynamic MRM (based on PFG-TSE) were analyzed without any assumption about the flow profile. The results are presented in images with the following parameters: the amount of stationary water, the amount of flowing water, the volume flow, the averaged linear flow velocity, the cross-sectional area of flow and the relative phloem flow.

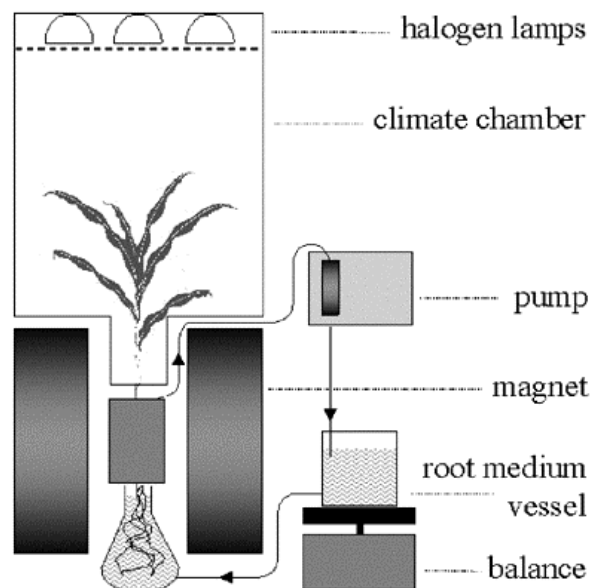


Fig. 2. Schematic drawing of the experimental set-up for an intact plant MRI study. The magnet used is an electromagnet.

This has been applied e.g. to study osmotic stress effects in intact drought sensitive maize and drought tolerant pearl millet plants, as well as the occurrence and repair of air embolism in xylem vessels. Xylem cavitation in the stem of cucumber plants (about 1.5 m height) was induced by cooling the roots for a period of three hours. Water uptake was measured with a weight balance simultaneously with the MRM experiments. The climate around the shoot of the plant was under full control by a climate chamber (Fig. 2).

Longitudinal NMR R_2 ($=1/T_2$) images of the shoot apex zone of a maize plant are shown in Fig. 3. The developing shoot with nodes, internodes, ear and surrounding leaves are clearly visible. Both in maize and pearl millet plants each internode has its specific T_2 value, which turned out to be uniquely correlated to the cell dimensions as determined by optical microscopy, with a correlation factor reflecting the membrane permeability for protons. This observation can be explained in the following way. The observed T_2 originates mainly from water in the vacuole, which occupies around 90 % of the water in the cells. For water in the vacuole exchange over the plasmalemma and the tonoplast membrane affects the observed relaxation. Due to the low S/N multi-exponential analysis per pixel was not successful, and therefore discrimination of water in the vacuole and cytoplasm was not.

Mild osmotic stress inhibited growth strongly in both maize (drought susceptible) and pearl millet (less susceptible), whereas the water uptake was far less affected. Hardly any changes in water content or T_2 in the stem region of maize were observed. In contrast, pearl millet showed a decrease in T_2 in the apical zone within 48 hours of stress. The cell

dimensions in the different internodes did not change as a function of stress (results of optical microscopy and cryo-SEM). In addition, it is very unlikely that the T_2 value of the bulk water in the vacuole changes in this amount (Clark et al, 1998). It was concluded that for maize, the water membrane permeability did not change during stress, whereas in pearl millet an increase of 35% was observed. We speculate that aquaporines (water channel forming proteins) play an important role in this increase.

The results of fast dynamic MRM can be presented in images with the following

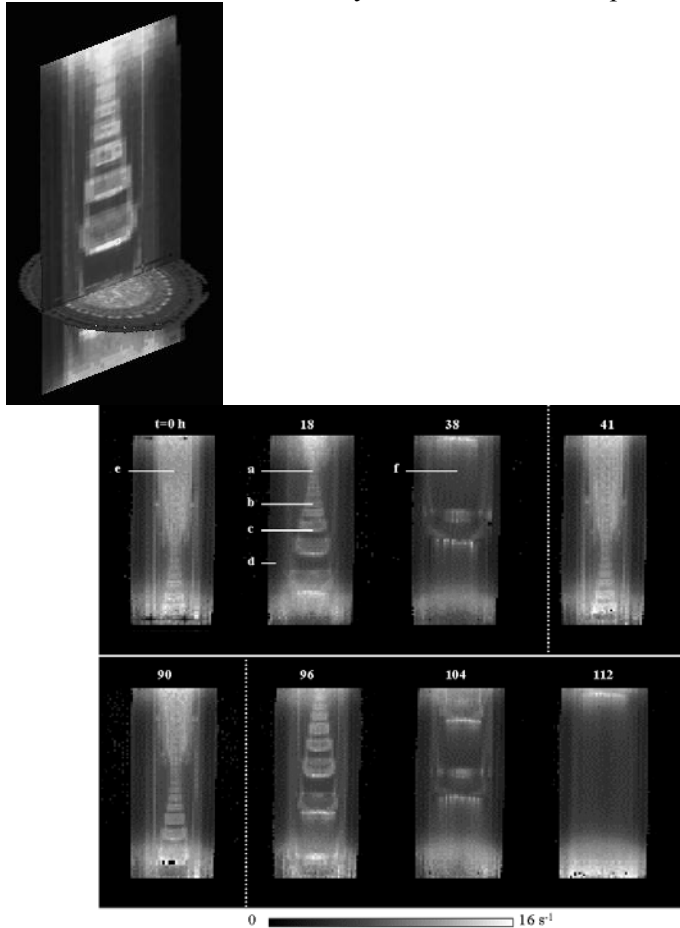


Fig. 3. A. Longitudinal and transversale R_2 images of the apex zone of intact maize plant. B. Time series of longitudinal images of the same plant. In the period between the dotted lines osmotic stress was applied by adding PEG to the root medium. Before doing so the position of the plant in the NMR rf coil was re-adjusted. In this way the effect on stress on the growth of the stem and adaptation of tissue in the apex zone could be studied.

parameters: the total amount of water, the amount of stationary water, the cross-sectional area of flow, the averaged linear flow velocity, and the volume flow. An example for cross-sectional images of the stem of a cucumber plant is given in Figure 4.

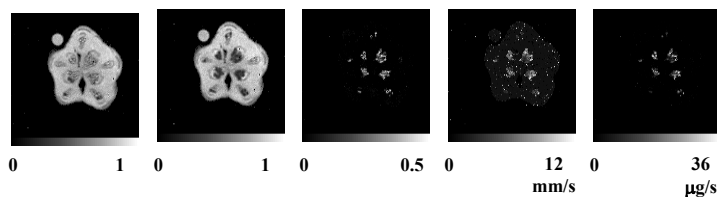


Fig. 4.

In the cucumber plants root cooling inhibited water uptake and resulted in a decrease of the cross-sectional area of flow, indicating the induction of embolisms. In one of our measurements some xylem vessels cavitated in the measured slice: some pixels in the vascular bundles completely lost intensity in all images after two to three hours of cooling. The leaves of the plant at that time were wilted. When cooling was relieved, water uptake restored partially and all leaves completely recovered within one hour (even under transpiring conditions). The visible embolisms in the images started refilling after about four hours, except from the very first embolized vessels: sixteen hours after cooling was relieved they still were not refilled.

The T_2 of parts of the parenchyma tissue decreased by about 40% at the time embolisms were visible. Per pixel only mono-exponential decay could be observed. On the basis of the differences in the T_2 values for the different tissues within the Cucumber stem selections of these different tissues could be made. Adding all decay curves within each selection greatly improved the S/N and a bi-exponential decay resulted as best fit. In this way the fraction and T_2 of water in the vacuole and cytoplasm could be discriminated and changes in time during the experiment could be revealed. In all selected tissues the water fractions (relative and absolute) were about constant. In the outer parenchyma the T_2 of both vacuole and cytoplasm was also constant, but in the inner parenchyma surrounding the vascular bundles and in the xylem parenchyma within the vascular bundles changes in T_2 in response to the root cooling were clearly observed. This again strongly points to a change in water permeability of the tonoplast, without changes in the distribution and amount of water in the two cell compartments.

Spatial and temporal resolution

In terms of spatial resolution, MRI is a relatively poor microscope. The spatial resolution (pixel dimension) that can be obtained depends on the magnetic field strength, B_0 , the radius of the rf measuring coil (detector), r , and details of the experimental parameters:

$$S/N \propto V B_0^{7/4} \Delta f^{-1} r^{-1} \sqrt{N_{av}} \sqrt{N_{echo}}$$

Here V is the pixel volume, N_{av} the number of averages, N_{echo} the number of echoes used to construct or calculate the image. Δf is the spectral width, representing the frequency range over the given field-of-view (FOV). It is inversely related to the dwell time, DW , the time between successive sampled data points.

A number of different approaches can be followed to increase the spatial resolution (minimal V) at a certain S/N, at the same time trying to avoid increasing the measurement time. The first gain can be obtained by optimizing r with respect to (part of) the object to be measured. The smaller r , the smaller pixel volume. Secondly, one can use high B_0 values. For plant tissues with extra-cellular air spaces this results in increased susceptibility artifacts. These artifacts can be overcome by increasing Δf , which results in a decrease in S/N. In addition, T_2 information as presented above is lost, because of an increased diffusion weighting in the echo amplitudes (Eqs 1 and 3). In fact, this effect becomes already significant at pixel dimensions smaller than about 100 μm . At higher B_0 the effective T_2 is (much) shorter than at lower field strength, limiting the number of measurable echoes (N_{echo}), again resulting in lower S/N.

Spatial resolution can also be increased by increasing N_{av} , but this reduces the temporal resolution strongly. Especially for displacement imaging this is a serious problem. For a reliable determination of $P_s(R, \Delta)$, the NMR signal (echo envelope) has to be measured as a function of minimal 32 different gradient values. It is clear that this takes time. A two dimensional SE image consisting of $N \times N$ pixels requires N acquisitions to be repeated. Combining this with displacement measurements with 64 gradient steps results in $64 \times N$ acquisitions. Doing so is very time consuming (several hours). Alternatively, displacement imaging has been combined with fast imaging techniques. For turboSE this results in a N/m times faster sequence as compared to a standard $N \times N$ SE image sequence. Here m is the

turbo factor, equal to the number of echoes that can be acquired in one scan. It is clear that the number of pixels, N , directly determines both spatial and temporal resolution.

An illustration of low field microscopy by use of optimized hardware is presented in Fig. 5. In this figure the effect of loss of information in T_2 due to diffusion effects at increasing resolution is also clearly visible.

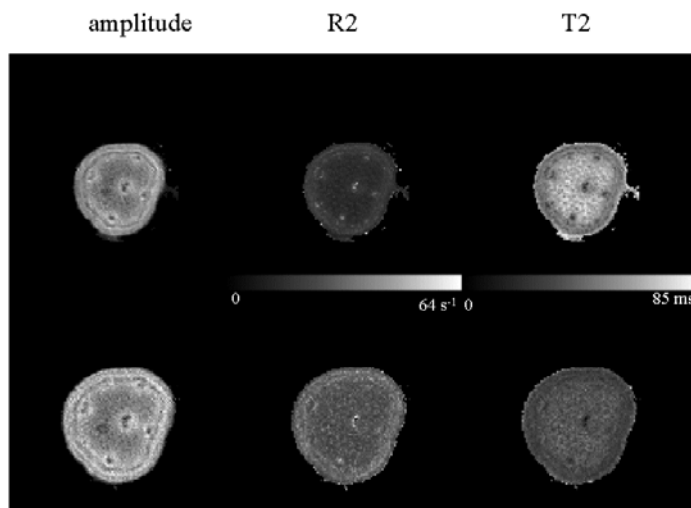


Fig. 4. Micro-images of leaf petiole of geranium measured with a small rf coil (i.d. 3 mm) at 30 MHz. Parameters: 25 kHz bandwidth, TE 6.6 ms, 128 x 128 x 16 matrix, FOV 5 en 4 mm (resolution 39*39*2500 and 31*31*2500 μm , resp.), 6 averages, TR 2.5 s, 32 minutes acquisition time.

Future

Functional imaging by dynamic MRI offers exciting new possibilities for the physiological mapping of whole plants to a high spatial and temporal resolution. For the first time, NMR imaging allows to describe the physiological state of individual plant organs and their inter-relationship at the whole plant level. Understanding plant physiology at this level will allow many as yet unanswered questions about plant productivity, development and stress responses to be answered, and open up unsurpassed new ways for understanding the relationships between growth, productivity, stress tolerance and competitiveness of plants. In addition, functional MRI is expected to be a powerful tool to characterise functionality of gene-expression by allowing to study protein action.

Literature:

1. Walter et al, 1992. Studies of plant systems by in vivo NMR spectroscopy. In "Magnetic Resonance Spectroscopy in Biology and Medicine", J.D. de Certaines, W.M.M.J. Bovée, F. Podo, eds. pp 573-610, Pergamon Press, Oxford.
2. Ratcliffe, 1994. In vivo NMR studies of higher plants and algae. *Advance in Botanical Research* 20:43-123.
3. MacFall and Van As, 1996. Magnetic resonance imaging of plants. In: *Nuclear magnetic resonance in plant biology* (Pfeffer and Shachar-Hill, eds.) *Am. Soc. Plant Physiol.*, pp. 33 - 69.
4. Chudeck and Hunter, 1997. Magnetic resonance imaging of plants. *Prog. Nucl. Magn. Reson. Spectrosc.* 31:43-62.
- Ishida, Koizumi and Kano, 2000. The NMR Microscope: a unique and promising tool for plant sciences. *Annals of Botany* 86: 259-278.
5. Kockenberger, 2001. *Trends in Plant Sciences*.